
GLOBAL OPTIMIZATION OF GRAPH ACQUISITION FUNCTIONS FOR NEURAL ARCHITECTURE SEARCH

Yilin Xie, Shiqiang Zhang, Jixiang Qing, Ruth Misener, Calvin Tsay*
 Department of Computing, Imperial College London
 London, United Kingdom

ABSTRACT

Graph Bayesian optimization (BO) has shown potential as a powerful and data-efficient tool for neural architecture search (NAS). Most existing graph BO works focus on developing graph surrogates models, i.e., metrics of networks and/or different kernels to quantify the similarity between networks. However, the acquisition optimization, as a discrete optimization task over graph structures, is not well studied due to the complexity of formulating the graph search space and acquisition functions. This paper presents explicit optimization formulations for graph input space including properties such as reachability and shortest paths, which are used later to formulate graph kernels and the acquisition function. We theoretically prove that the proposed encoding is an equivalent representation of the graph space and provide restrictions for the NAS domain with either node or edge labels. Numerical results over several NAS benchmarks show that our method efficiently finds the optimal architecture for most cases, highlighting its efficacy.

1 Introduction

Despite numerous breakthroughs in deep learning, the design of neural architectures largely relies on prior experience and heuristic search. Moreover, the neural architecture design underlies the learned representation of the data, and the ultimate downstream performance in predictive tasks. The field of neural architecture search (NAS) seeks to automate this key step, by letting algorithms automatically design the architecture of a neural network model (Ren et al., 2021). In general, NAS algorithms share several steps (Salmani Pour Avval et al., 2025): (i) encoding the search space, e.g., as a general or modular domain, (ii) prescribing a search strategy over the above space, and (iii) assessing the (approximate) performance at selected points. Early works in NAS sought to encode a general search space from scratch, e.g., as a string (Zoph and Le, 2017). Later works constrain the search space toward problem tractability, such as by explicitly encoding a layer- or module-based structure (Liu et al., 2018; Wu et al., 2019). Search strategies are often based on random search, gradient-based optimization (Liu et al., 2019; Wu et al., 2019), Bayesian optimization (White et al., 2021a; Ru et al., 2021), evolutionary algorithms (Real et al., 2019; Qiu et al., 2023), or reinforcement learning (Zoph and Le, 2017; Jaafra et al., 2019; Cheng et al., 2022). Finally, performance assessments are the most expensive step of NAS, often involving full or partial training of the proposed model(s).

Graph Bayesian optimization (BO) exhibits state-of-the-art performance in NAS (Elsken et al., 2019; White et al., 2023), given the ability of algorithms to efficiently explore the graph search space and identify promising architectures within limited budgets (Ru et al., 2021). Graph BO addresses the above NAS steps using (i) a graph surrogate that is trained over available data and then serves as a predictor, and (ii) an acquisition function, encoding trade-offs between exploitation and exploration, that is optimized to propose the next candidate. From modeling perspectives, Gaussian processes (GPs) (Schulz et al., 2018) are commonly used since they offer accurate prediction along with uncertainty quantification. To apply GPs in a graph domain, graph kernels (Vishwanathan et al., 2010; Borgwardt et al., 2020; Kriege et al., 2020; Nikolentzos et al., 2021) are introduced to measure the similarity between graphs. Although advances in graph kernels facilitate the generalization from non-structural spaces to graph space, optimizing acquisition functions over (combinatorial) graph spaces remains a challenge. Most works use sample-based or evolutionary algorithms, since they only require evaluations of the acquisition function and can thus be easily applied to various graph domains.

*Corresponding author: c.tsay@imperial.ac.uk

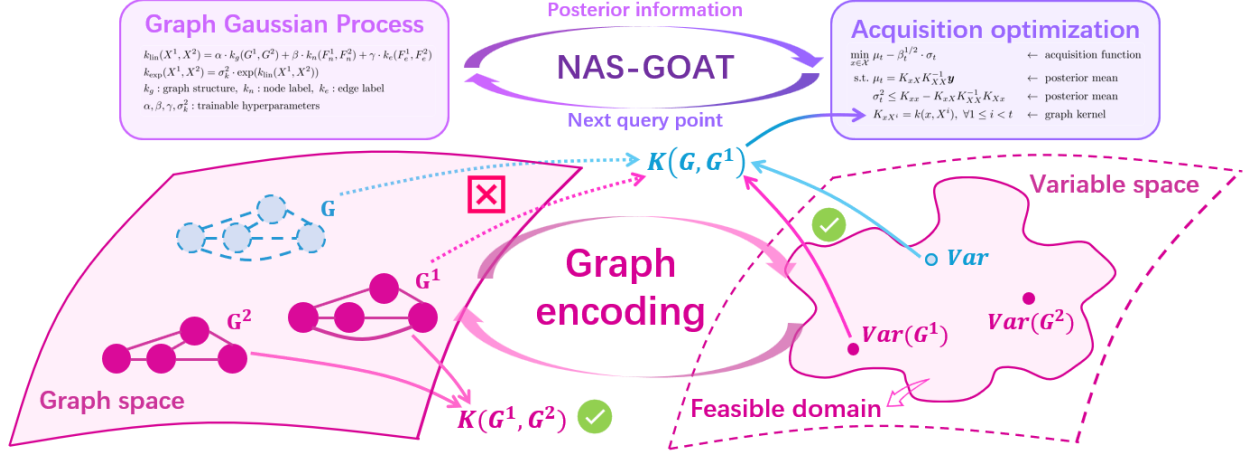


Figure 1: Illustration of NAS-GOAT. The main idea is to represent graphs in variable space and introduce constraints to build a bijection between all graphs and the feasible domain. The graph kernel value between an unknown graph (which is our optimization target) and a given graph is then formulated as expressions of variables, or constraints, enabling us to employ global optimization for acquisition function and propose the next neural architecture to evaluate.

However, these algorithms must incorporate problem-specific constraints into the sampling and mutation steps to remove invalid candidates, and there is no theoretical guarantee about the optimality of solutions obtained from these methods.

Recently, the idea of using mathematical programming techniques to formulate machine learning (ML) models, e.g., neural networks (NNs) (Fischetti and Jo, 2018; Anderson et al., 2020; Tsay et al., 2021; Zhang et al., 2023), trees (Mišić, 2020; Mistry et al., 2021; Ammari et al., 2023), and GPs (Schweidtmann et al., 2021; Xie et al., 2024), has attracted a lot of attention, since it provides a way to explicitly solve decision-making problems involving ML models. Relevant applications include BO acquisition optimization Thebelt et al. (2021, 2022); Wang et al. (2023), NN verification (Huchette et al., 2023; Hojny et al., 2024), molecular design (Zhang et al., 2024; McDonald et al., 2024), among others. Based on the global optimization formulation for acquisition optimization proposed in (Xie et al., 2024), Xie et al. (2025) propose BoGrape as a general graph BO framework, comprising the first work to treat graph acquisition functions from a discrete optimization viewpoint. By encoding graph spaces and shortest-path graph kernels (Borgwardt and Kriegel, 2005) into mixed-integer programming (MIP), BoGrape can handle constraints over graph search spaces and globally optimize the acquisition function with theoretical guarantees. However, the requirement of strong connectivity makes BoGrape unsuitable for NAS, since neural architectures are weakly connected acyclic digraphs (DAGs).

This paper studies the global optimization of graph acquisition functions for graph BO-based NAS. To represent the graph space containing valid neural architectures, we generalize the graph encoding presented in Xie et al. (2025) to omit assumptions about connectivity, and we show how the resulting general encoding can be restricted to the NAS search space. GPs with shortest-path kernels are used as graph surrogates, and lower confidence bound (LCB) (Srinivas et al., 2010) is chosen as the acquisition function. The proposed graph encoding contains graph properties including reachability and shortest paths and is therefore compatible with existing formulations for shortest-path graph kernels and acquisition functions (Xie et al., 2025). The final acquisition optimization is formulated as a MIP, which can be solved by MIP solvers with global optimality guarantees. Figure 1 illustrates the main idea of the proposed framework, we also list the major contributions of this work are as follows:

- We present an equivalent representation for general labeled graphs in variable space. Each graph corresponds to a unique feasible solution containing its graph structure, as well as graph properties including reachability, shortest distances, and shortest paths.
- We provide a general kernel form measuring the similarity between two labeled graphs over graph structure, node label, and edge label levels, and we present a formulation that is compatible with our graph encoding.
- We incorporate NAS-specific constraints to the graph encoding, which define the valid search space for the NAS task using either node labels or edge labels.
- We propose NAS-GOAT to globally optimize graph acquisition functions based on our proposed encoding. Numerical results demonstrating a full BO loop on NAS benchmarks show the efficiency and potential of NAS-GOAT.

Paper structure: Section 2 provides preliminary knowledge. Section 3 introduces our methodology and theoretical results. Section 4 reports the experimental results. Section 5 concludes this work and discusses the future work. Appendices contain all proofs and further details.

2 Background

2.1 Cell-based NAS

In many NAS search spaces, a network architecture is designed by varying some repeated small feedforward sub-structures called cells (Ying et al., 2019; Dong and Yang, 2020). Each cell is treated as a DAG, where the operation units are represented as node or edge labels, and information flows within the cell following graph topologies. Cells are then stacked multiple times and embedded into a macro neural network ‘skeleton’ to give the final architecture. For instance, NAS-Bench-101 (Ying et al., 2019) and NAS-Bench-201 (Dong and Yang, 2020) define one stack as 3 and 5 replications of cells, resp., and each stack appears 3 times in the overall network structure. Cell-based NAS can be naturally considered as an expensive black-box optimization problem, where one aims to search for the best graph, i.e., cell, that optimizes the performance of the resulting neural architecture over certain metrics, e.g., validation/test accuracy.

2.2 Graph Bayesian optimization

Graph BO is a natural extension of BO (Frazier, 2018; Garnett, 2023) from vector space to graph space. At the t -th iteration, a graph Gaussian process (GP) equipped with a graph kernel is trained on available data $X = \{(G^i, F^i), y^i\}_{i=1}^{t-1}$. The posterior mean $\mu_t(\cdot)$ and variance $\sigma_t^2(\cdot)$ obtained from the graph GP are used to define acquisition functions such as lower confidence bound (LCB): $\alpha_{LCB}(x) = \mu_t(x) - \beta_t^{1/2} \cdot \sigma_t(x)$, where β_t is a hyperparameter balancing between exploitation and exploration.

From modeling perspectives, the core component of graph GPs is the graph kernels that measure the similarity between graphs. Classic graph kernels include random walk (RW) (Gärtner et al., 2003), subgraph matching (SM) (Kriege and Mutzel, 2012), shortest-path (SP) (Borgwardt and Kriegel, 2005), Weisfeiler-Lehman (WL) (Shervashidze et al., 2011), and Weisfeiler-Lehman optimal transport (WLOA) (Kriege et al., 2016) kernels; we refer the reader to Vishwanathan et al. (2010); Borgwardt et al. (2020); Kriege et al. (2020); Nikolentzos et al. (2021) for comprehensive details about graph kernels. In this work, we consider SP kernels used for graph BO in (Xie et al., 2025). Mathematically, for two node labeled graphs G^1 and G^2 , denote V^1 and V^2 as their node sets, resp., l_v as the label of v , and $d_{u,v}$ as the shortest distance from node u to node v . The SP kernel is defined as:

$$k_{SP}(G^1, G^2) = \frac{1}{n_1^2 n_2^2} \sum_{u_1, v_1 \in V^1, u_2, v_2 \in V^2} \mathbf{1}(l_{u_1} = l_{u_2}) \cdot \mathbf{1}(d_{u_1, v_1} = d_{u_2, v_2}) \cdot \mathbf{1}(l_{v_1} = l_{v_2}), \quad (k_g)$$

where $n_1^2 n_2^2$ is a normalizing coefficient with n_1 and n_2 as the node number of G^1 and G^2 , resp.

2.3 Graph acquisition optimization

The major challenge of graph BO is the acquisition optimization, which seeks to find the graph structure with optimal acquisition function value and is often required for convergence proofs. Encoding a graph search space and acquisition function as optimization constraints is non-trivial, and most existing works follow a sample-then-evaluate procedure to avoid directly optimizing over discrete space, e.g., (Kandasamy et al., 2018; Ru et al., 2021; Wan et al., 2021, 2023). From a discrete optimization viewpoint, Xie et al. (2025) first formulate graph space and shortest-path graph kernels using MIP, and propose BoGrape as a graph BO framework that can globally optimize the lower confidence bound (LCB) acquisition:

$$\begin{aligned} \min_{x \in \mathcal{X}} \quad & \mu_t - \beta_t^{1/2} \cdot \sigma_t && \leftarrow \text{acquisition function} \\ \text{s.t.} \quad & \mu_t = K_{xX} K_{XX}^{-1} \mathbf{y} && \leftarrow \text{posterior mean} \\ & \sigma_t^2 \leq K_{xx} - K_{xX} K_{XX}^{-1} K_{Xx} && \leftarrow \text{posterior mean} \\ & K_{xX^i} = k(x, X^i), \forall 1 \leq i \leq t && \leftarrow \text{graph kernel} \end{aligned} \quad (\text{Acq-Opt})$$

However, graphs considered in (Xie et al., 2025) are assumed to be strongly connected and have node labels, while graphs involved in NAS are weakly connected graphs, probably with edge labels.

3 Methodology

3.1 Encoding a graph search space in optimization

Firstly and most importantly, we must properly define the graph search space over which acquisition optimization is performed. In this section, we temporarily ignore node/edge features and focus on graph structures. To avoid graph isomorphism caused by node indexing, we assume that all nodes are labeled differently. Intuitively, encoding such a general graph space is easy, since each graph is uniquely determined by its adjacency matrix, and one only needs to define the $n \times n$ adjacency matrix containing binary variables $A_{u,v}$ that denote the existence of edge $u \rightarrow v$. However, this naive encoding has no extra graph information, e.g., connectivity, reachability, shortest distance, which are important for defining acquisition functions and feasible graphs. Encoding these graph properties into decision space is significantly more challenging because we must define constraints that prescribe all variables to have correct values for *any* possible graph in the search space.

The graph encoding introduced in this paper incorporates reachability, shortest distances, and shortest paths for any graph without requiring strong connectivity as in previous work (Xie et al., 2024). These metrics are then used to encode shortest-path graph kernels for graph BO. To begin with, we define variables corresponding to relevant graph properties in Table 1. We consider all graphs with node number ranging from n_0 to n . For simplicity, we use $[n]$ to denote the set $\{0, 1, \dots, n-1\}$.

For each variable Var in Table 1, we use $Var(G)$ to denote its value on a given graph G . For example, $d_{u,v}(G)$ is the shortest distance from node u to node v in graph G . If graph G is given, all variable values can be easily obtained using classic shortest-path algorithms, such as the Floyd–Warshall algorithm (Floyd, 1962). However, for optimization over graphs, the variables must be constrained properly so that they take correct values for any given graph, i.e., to match the Description column in Table 1. Due to space limitations, we only present the final derived encoding in Eq. (Graph-Encoding) and the major theory in Theorem 1. Full derivations are given in Appendix A.

Eq. (Graph-Encoding) comprises many linear constraints resulting from Conditions (C1)–(C8), as shown in Appendix A.1. Here we present the final formulation, which conveys the overall idea about how to use constraints to mathematically define variables over graphs. Constraints for optimization formulations must be carefully selected. There are often multiple ways to encode a combinatorial problem, but insufficient constraints result in an unnecessarily large search space with symmetric solutions, while excessive constraints may cutoff feasible solutions from the search space. Theorem 1 guarantees that our encoding precisely formulates the graph space (see Appendix A.2 for proofs).

Theorem 1. *There is a bijection between the feasible domain restricted by Eq. (Graph-Encoding) with size $[n_0, n]$ and the whole graph space with node numbers in $[n_0, n]$.*

The encoding proposed in (Xie et al., 2025) requires connected undirected graphs or strongly connected directed graphs, while our encoding Eq. (Graph-Encoding) is more general and formulates the whole graph space without connectivity requirements. Observe that our encoding Eq. (Graph-Encoding) can be easily restricted to the encoding in (Xie et al., 2025) by adding the following constraints:

Undirected: Add symmetry constraints to get undirected graphs:

$$A_{u,v} = A_{v,u}, r_{u,v} = r_{v,u}, d_{u,v} = d_{v,u}, \delta_{u,v}^w = \delta_{v,u}^w, \forall u, v, w \in [n], u < v.$$

Strong connectivity: Each existing node can reach all other existing nodes, i.e.,

$$A_{u,u} = A_{v,v} = 1 \Rightarrow r_{u,v} = 1, \forall u, v \in [n], u \neq v,$$

which can be equivalently rewritten as the following constraint:

$$r_{u,v} \geq A_{u,u} + A_{v,v} - 1, \forall u, v \in [n], u \neq v.$$

Remark 1. *Note that strong connectivity reduces to connectivity for undirected graphs.*

Table 1: Variables introduced to encode shortest paths for an arbitrary graph. Since the shortest distance between two nodes is always less than n , we use n to denote infinity, i.e., $d_{u,v} = n$ means node u cannot reach node v .

Variables	Domain	Description
$A_{v,v}, v \in [n]$	$\{0, 1\}$	if node v exists
$A_{u,v}, u, v \in [n], u \neq v$	$\{0, 1\}$	if edge $u \rightarrow v$ exists
$r_{u,v}, u, v \in [n]$	$\{0, 1\}$	if node u can reach node v
$d_{u,v}, u, v \in [n]$	$[n+1]$	the shortest distance from node u to node v
$\delta_{u,v}^w, u, v, w \in [n]$	$\{0, 1\}$	if node w appears on the shortest path from node u to node v

$$\left\{ \begin{array}{l}
 \sum_{v \in [n]} A_{v,v} \geq n_0 \\
 A_{v,v} \geq A_{v+1,v+1} \\
 2 \cdot A_{u,v} \leq A_{u,u} + A_{v,v} \\
 2 \cdot r_{u,v} \leq A_{u,u} + A_{v,v} \\
 d_{u,v} \geq n \cdot (1 - A_{u,u}) \\
 d_{u,v} \geq n \cdot (1 - A_{v,v}) \\
 r_{v,v} = 1 \\
 d_{v,v} = 0 \\
 \delta_{v,v}^v = 1 \\
 \delta_{v,v}^w = 0 \\
 r_{u,v} \geq A_{u,v} \\
 d_{u,v} \geq 2 - A_{u,v} \\
 d_{u,v} \leq 1 + (n-1) \cdot (1 - A_{u,v}) \\
 d_{u,v} \leq n - r_{u,v} \\
 d_{u,v} \geq n - (n-1) \cdot r_{u,v} \\
 r_{u,w} + r_{w,v} \geq 2 \cdot \delta_{u,v}^w \\
 r_{u,v} \geq r_{u,w} + r_{w,v} - 1 \\
 \delta_{u,v}^u = \delta_{u,v}^v = 1 \\
 \sum_{w \in [n]} \delta_{u,v}^w \geq 2 + r_{u,v} - A_{u,v} \\
 \sum_{w \in [n]} \delta_{u,v}^w \leq 2 + (n-2) \cdot (r_{u,v} - A_{u,v}) \\
 d_{u,v} \leq d_{u,w} + d_{w,v} - (1 - \delta_{u,v}^w) + (n+1) \cdot (2 - r_{u,w} - r_{w,v}) \\
 d_{u,v} \geq d_{u,w} + d_{w,v} - 2n \cdot (1 - \delta_{u,v}^w)
 \end{array} \right. \quad (\text{Graph-Encoding})$$

3.2 Restricting search space to the NAS domain

The graphs considered in NAS are acyclic digraphs (DAGs), which are straightforward for formulate by adding the following constraints to Eq. (Graph-Encoding):

$$r_{u,v} + r_{v,u} \leq 1, \forall u, v \in [n], u < v.$$

In practice, however, the graph structures are more specific, e.g., having a single source (input) and single sink (output), and each graph may include node/edge labels. We consider DAGs with one source and one sink, which is the most classic setting in cell-based NAS. Based on the label type, we investigate two scenarios, i.e., node-labeled and edge-labeled DAGs, corresponding to the most commonly used benchmarks NAS-Bench-101 and NAS-Bench-201, resp.

Node-labeled DAGs: Following the NAS-Bench-101 (Ying et al., 2019) setting, we consider DAGs with n nodes, at most E edges, and L_n different node labels (including two extra labels to identify the source and the sink). W.l.o.g., we use the first label for the source, and the last label for the sink. Introducing variable $F_{v,l} \in \{0, 1\}$ to represent whether

node $v \in [n]$ has label $l \in [L_n]$, we can write:

$$\begin{aligned} & \begin{cases} A_{u,v} = 0, r_{u,v} = 0, d_{u,v} = n, \delta_{u,v}^w = 0, \forall u, v, w \in [n], u > v, w \neq u, v \end{cases} & (1a) \\ & \begin{cases} r_{0,v} = 1, F_{0,0} = 1, F_{v,0} = 0, \forall v \in [n], v \neq 0 \end{cases} & (1b) \\ & \begin{cases} r_{v,n-1} = 1, F_{n-1,L_n-1} = 1, F_{v,L_n-1} = 0, \forall v \in [n], v \neq n-1 \end{cases} & (1c) \\ & \begin{cases} \sum_{l \in [L_n]} F_{v,l} = 1, \forall v \in [n] \end{cases} & (1d) \\ & \begin{cases} \sum_{u < v} A_{u,v} \leq E \end{cases} & (1e) \end{aligned}$$

Eq. (1a) enforces that each edge starts from the node with smaller index to reduce the number of isomorphic graphs. Eq. (1b) sets node 0 as the source, from which every other node can be reached. Eq. (1c) sets node $(n-1)$ as the sink, which every other node can reach. Eq. (1d) enforces each node to take one label, and Eq. (1e) limits the maximal number of edges.

Remark 2. *NAS-Bench-101 is a particular instance of the above, i.e., with $n = 7$, $E = 9$, $L_n = 5$.*

Edge-labeled DAGs: Following the NAS-Bench-201 (Dong and Yang, 2020) and DARTS settings, we consider DAGs with n nodes (meaning all nodes are already indexed) and L_e edge labels. Introducing variable $F_{u \rightarrow v, l}$ to represent whether edge $u \rightarrow v$ (with $u < v$) has label $l \in [L_e]$, we have the encoding:

$$\begin{aligned} & \begin{cases} A_{u,v} = 0, r_{u,v} = 0, d_{u,v} = n, \delta_{u,v}^w = 0, \forall u, v, w \in [n], u > v, w \neq u, v \end{cases} & (2a) \\ & \begin{cases} r_{0,v} = r_{v,n-1} = 1, \forall v \in [n] \end{cases} & (2b) \\ & \begin{cases} \sum_{l \in [L_e]} F_{u \rightarrow v, l} = A_{u,v}, \forall u, v \in [n], u < v \end{cases} & (2c) \end{aligned}$$

Eq. (2a) is the same as Eq. (1a), Eq. (2c) sets node 0 as the source and node $(n-1)$ as the sink, and Eq. (2c) forces one edge label for each existing edge and no edge labels for nonexistent edges.

Remark 3. *NAS-Bench-201 is a particular instance of the above, i.e., with $n = 4$, $L_e = 4$. Note that NAS-Bench-201 has 5 labels: one label denotes nonexistence, which is not needed in our encoding.*

3.3 Encode graph kernels

We take the triple (G, F_n, F_e) as a graph with node labels $F_n = \{F_{v,l}\}_{v \in [n], l \in [L_n]}$ and edge labels $F_e = \{F_{u \rightarrow v, l}\}_{u, v \in [n], l \in [L_e]}$. Given two labeled graphs $X^1 = (G^1, F_n^1, F_e^1)$ and $X^2 = (G^2, F_n^2, F_e^2)$ and denoting their node numbers as n_1 and n_2 , resp., we define the following general kernel form:

$$k_{\text{lin}}(X^1, X^2) = \alpha \cdot k_g(G^1, G^2) + \beta \cdot k_n(F_n^1, F_n^2) + \gamma \cdot k_e(F_e^1, F_e^2), \quad (\text{linear})$$

where kernels k_g, k_n, k_e quantify similarity over graph structure, node labels, and edge labels, resp.

We then denote the optimization target as an unknown graph $x = (G, F_n, F_e)$, and the available data points as $X = \{X^i, y^i\}_{i=1}^{t-1}$ with $X^i = (G^i, F_n^i, F_e^i)$. After properly defining the search space in Section 3.2, the last step is to encode kernel-relevant terms in Eq. (Acq-Opt), i.e., k_{xX^i} and k_{xx} . For graph structure G and node labels F_n , the encoding of the graph structure (k_g) kernel, i.e., $k_g(G, G), k_g(G, G^i)$ and binary node features, i.e., $k_n(F_n, F_n), k_n(F_n, F_n^i)$ are given in (Xie et al., 2025). For completeness, we provide details in Appendix B.

Edge label encoding: Edge labels can be treated in a similar way to node labels. However, several NAS settings have more specific properties, i.e., all nodes are indexed when edge labels are present, and all graphs have the same size. Thus we alternatively propose the following simplified form:

$$k_e(F_e^1, F_e^2) = \frac{2}{n(n-1)} \langle F_e^1, F_e^2 \rangle = \frac{2}{n(n-1)} \sum_{u < v} \sum_{l \in [L_e]} F_{u \rightarrow v, l}^1 \cdot F_{u \rightarrow v, l}^2, \quad (k_e)$$

where $n(n-1)/2$ is a normalizing coefficient, with n as the node number of both G^1 and G^2 , given that a DAG has at most $n(n-1)/2$ edges.

We take edge kernels as follows, and evaluate their performance in Section 4.3:

$$\begin{aligned} k_e(F_e, F_e^i) &= \frac{2}{n(n-1)} \sum_{u < v} \sum_{l \in [L_e]} F_{u \rightarrow v, l}^i \cdot F_{u \rightarrow v, l}, \\ k_e(F_e, F_e) &= \frac{2}{n(n-1)} \sum_{u < v} \sum_{l \in [L_e]} F_{u \rightarrow v, l}^2 = \frac{2}{n(n-1)} \sum_{u < v} \sum_{l \in [L_e]} F_{u \rightarrow v, l} = \frac{2}{n(n-1)} \sum_{u < v} A_{u,v}, \end{aligned}$$

Table 2: NAS algorithms comparison, including whether the method is BO-based, the surrogate model used, and how acquisition function is optimized (if BO-based). The superscript ‘^a’ denotes methods that are not originally designed for NAS but can be adapted for NAS settings. For surrogate models, we use ‘v’ to denote models using vectorized embeddings of graphs and ‘g’ to denote models that directly over graph spaces.

Algorithms	BO-based	Surrogate	Acquisition optimization
Random	×	-	-
DNGO ^a (Snoek et al., 2015)	✓	BNN(v)	mutation
BOHAMIANN ^a (Springenberg et al., 2016)	✓	BNN(v)	mutation
NASBOT (Kandasamy et al., 2018)	✓	GP(g)	mutation
Evolution (Real et al., 2019)	×	-	-
GP-BAYESOPT ^a (Neiswanger et al., 2019)	✓	GP(v)	sampling
GCN (Wen et al., 2020)	×	-	-
BONAS (Shi et al., 2020)	✓	GCN(v)	sampling
Local search (White et al., 2021b)	×	-	-
BANANAS (White et al., 2021a)	✓	NN(v)	mutation
NAS-BOWL (Ru et al., 2021)	✓	GP(g)	mutation
NAS-GOAT (ours)	✓	GP(g)	MIP

where we use the trick that $x^2 = x$ for binary x and the relation in Eq. (2c).

The above defines a formulation for all relevant terms in kernel form (linear). To improve representation ability, we also consider an alternative exponential form defined as Xie et al. (2025):

$$k_{\text{exp}}(X^1, X^2) = \sigma_k^2 \cdot \exp(k_{\text{lin}}(X^1, X^2)), \quad (\text{exponential})$$

where the variance σ_k^2 controls the magnitude of kernel values.

4 Experiments

All experiments are performed on a 4.2 GHz Intel Core i7-7700K CPU with 16 GB memory. For our methods, we use GPflow (Matthews et al., 2017) to implement GP models, and Gurobi (Gurobi Optimization, LLC, 2024) to solve MIPs. For kernel comparison, GraKel (Siglidis et al., 2020) is used to implement graph kernels. We use the published implementations of NAS-BOWL (Ru et al., 2021) and Naszilla (White et al., 2020, 2021b,a) for all other NAS baselines.

4.1 Benchmarks

We choose the most popular benchmarks used in NAS literature, i.e., NAS-Bench-101 (Ying et al., 2019) and NAS-Bench-201 (Dong and Yang, 2020), to evaluate the performance of our proposed method. These two benchmarks correspond to the node- and edge-labeled cases as discussed in Section 3.2, resp..

NAS-Bench-101: DAGs with one source, one sink, at most 7 nodes and 9 edges, and 3 different node operations. Only the source is labeled as operation IN, only the sink is labeled as operation OUT, and each of other nodes has one of the remaining three operations: 3x3 convolution, 1x1 convolution, or 3x3 max pooling. After removal of duplicates, NAS-Bench-101 has approximately 423k unique architectures. Each architecture is trained on CIFAR-10 to obtain validation and test accuracies.

NAS-Bench-201: Dense DAGs with 4 nodes. Each of the 6 edges has a label chosen from 5 operation types: zeroize, skip-connection, 1x1 convolution, 3x3 convolution, or 3x3 average pooling. NAS-Bench-201 has 15,625 architectures in total, each of which has various metrics including validation and test accuracies over three datasets: CIFAR10, CIFAR100, and ImageNet-16-120.

In both benchmarks, each architecture is trained 20 times with varying random seeds, which could be used as a noisy objective function as suggested in (Ru et al., 2021). We conduct experiments for both scenarios, reporting results for the deterministic setting here, i.e., averaging the accuracies over multiple random seeds. Results for noisy setting are given in Appendix C.

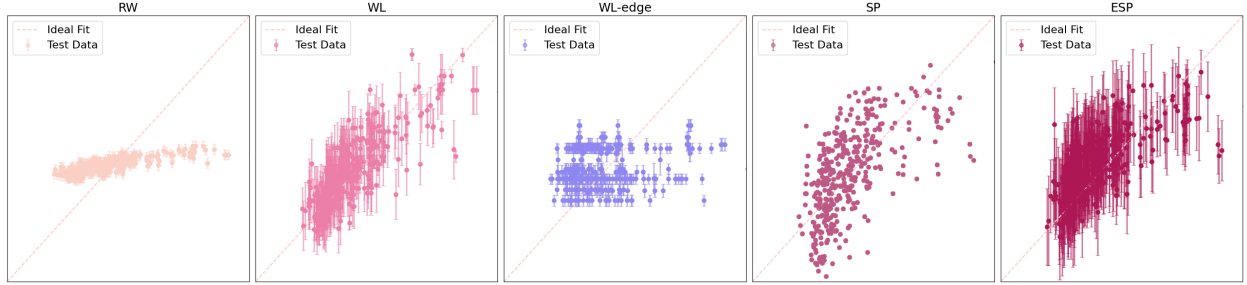


Figure 2: Predictive performance of graph GPs with different kernels. 50 and 400 architectures are randomly sampled from NAS-Bench-201 for training and testing, resp. Predicted deterministic validation error are plotted against the true values, with one standard deviation as error bars.

Table 3: GP model performance metrics using different graph kernels. For each dataset, 50 and 400 architectures are sampled for training and testing, resp. Predictive performance metrics are averaged over 20 replications and reported in the table, with one standard deviation in the brackets. The best method is marked in **bold** metric-wisely for each dataset.

Dataset	NAS-Bench-101			NAS-Bench-201		
Kernel	RMSE ↓	MNLL ↓	Spearman ↑	RMSE ↓	MNLL ↓	Spearman ↑
RW	0.29(0.01)	30.29(5.26)	0.81(0.04)	0.32(0.02)	43.07(19.14)	0.78(0.05)
WL	0.15(0.02)	-0.77(0.07)	0.87(0.03)	0.23(0.04)	0.98(1.02)	0.81(0.07)
WL-edge	-	-	-	0.37(0.02)	46.00(16.73)	0.11(0.09)
SP	0.21(0.05)	227.67(114.59)	0.83(0.04)	0.33(0.04)	465.15(152.20)	0.63(0.10)
ESP	0.11(0.02)	28.83(15.02)	0.93(0.02)	0.30(0.04)	0.36(0.22)	0.64(0.11)

4.2 Baselines

We compare our method, NAS-GOAT, which is capable of globally optimizing acquisition in form (Acq-Opt) with the encoding introduced in Section 3, against state-of-the-art baselines in NAS, summarized in Table 2. BO-based baselines either use GPs or neural predictors as the surrogate model. Graph inputs are featurized into vectors using different encoding methods before feeding to NN surrogates (Snoek et al., 2015; Springenberg et al., 2016; Shi et al., 2020; White et al., 2021a). For GP surrogate models, graphs can be directly used as data points by defining a proper graph kernel (Ru et al., 2021) or graph similarity metric (Kandasamy et al., 2018). In addition to BO-based algorithms, we also include classic methods in NAS such as random search (Random), regularized evolution (Evolution) (Real et al., 2019), local search (Local search) (White et al., 2021b) and GCN predictor (GCN) (Wen et al., 2020). For BO-based methods, optimization of acquisition functions is achieved through mutation or sampling, while NAS-GOAT is capable of globally acquisition optimization over graph search spaces. More descriptions and implementation details of the baselines can be found in Appendix C.

4.3 Graph kernels comparison

Although the focus of this paper is global acquisition optimization rather than graph modeling, the kernel performance is still important to overall BO performance, noting that we employ SP kernels. In this section, we compare the predictive performance of graph GPs equipped with various graph kernels. For NAS-Bench-101 with node labels, we compare RW, WL, and our kernels in form (linear) (SP) and (exponential) (ESP). For NAS-Bench-201 with edge labels, all architectures are first converted to node-labeled graphs and then evaluated over RW and WL kernels. We also test the performance of WL kernels over the original edge-labeled graphs (denoted as WL-e). Both SP and ESP kernels can directly handle edge labels without conversion.

Figure 2 illustrates the predictive performance of different kernels on NAS-Bench-201 (see Figure 4 in Appendix C for a similar plot for NAS-Bench-101), and Table 3 reports performance metrics including root mean squared error (RMSE) and Spearman’s rank correlation (Spearman) showing the predictive accuracy, as well as mean negative log likelihood (MNLL) measuring the uncertainty qualification. The RW kernel does not perform well on both cases. The WL kernel performs significantly better on converted node-labeled graphs compared to the original edge-labeled graphs, which matches the empirical observations in (Ru et al., 2021). WL and ESP kernels have comparably good performance, both of which outperform the SP kernel. Note that a better kernel may not necessarily translate to better optimization results,

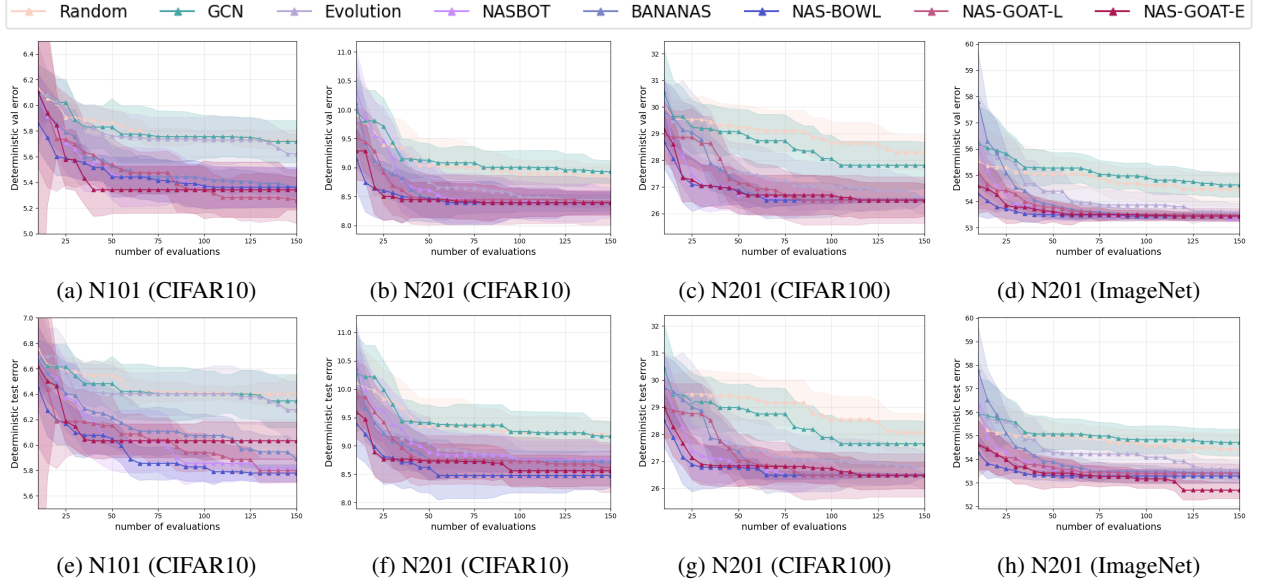


Figure 3: Numerical results of Graph BO on NAS-Bench-101 (N101) and NAS-Bench-201 (N201). (**Top**) Deterministic validation error. (**Bottom**) The corresponding test error. Median with one standard deviation over 20 replications is plotted.

since complex kernel forms bring extra difficulties in acquisition optimization, resulting in a computational trade-off between the modeling and optimization steps.

4.4 Graph BO for NAS

In this section, we test the performance of NAS-GOAT in a full BO loop over NAS benchmarks against baselines. Following the batch setting in White et al. (2021a); Ru et al. (2021), we conduct 30 BO iterations starting with 10 initial samples. At each iteration, we solve the MIP defined by Eq. (Graph-Encoding) using Gurobi Gurobi Optimization, LLC (2024) and store the best 5 candidates (in terms of acquisition function value) to evaluate.

We denote our methods as NAS-GOAT-L (using kernel (linear)) and NAS-GOAT-E (using kernel (exponential)) to differentiate the kernel used in graph GP. All baselines introduced in Table 2 are implemented, but we only report Random, GCN (Wen et al., 2020), Evolution (Real et al., 2019), NASBOT (Kandasamy et al., 2018), BANANAS (White et al., 2021a) and NAS-BOWL (Ru et al., 2021) here for conciseness, since they usually achieve better results. Full baselines are given in Appendix C. Following NAS literature, we minimize over validation error and report both validation and test errors. As shown in Figure 3, both NAS-GOAT-L and NAS-GOAT-E find (near-)optimal architectures in all scenarios. NAS-GOAT-L achieves slightly better performance perhaps owing to its simpler form, making the resulting optimization formulation less complicated.

5 Conclusion

This work considers global acquisition optimization in graph BO for NAS. The graph search space is precisely encoded into an equivalent variable space for discrete optimization. A general kernel is designed to handle both node and edge labels, and formulations are proposed based on the graph encoding. After adding suitable constraints to remove invalid architectures, we are able to globally optimize the acquisition function at each BO iteration, demonstrating promising results on commonly used NAS benchmarks. Future works could consider more graph kernels beyond shortest-path kernels, or apply the proposed method to more graph-based decision making problems.

Acknowledgments

The authors gratefully acknowledge support from a Department of Computing Scholarship (YX), BASF SE, Ludwigshafen am Rhein (SZ), Engineering and Physical Sciences Research Council [grant numbers EP/W003317/1 and EP/X025292/1] (RM, CT, JQ), a BASF/RAEng Research Chair in Data-Driven Optimisation (RM), a BASF/RAEng

Senior Research Fellowship (CT). RM holds concurrent appointments as a Professor at Imperial and as an Amazon Scholar. This paper describes work performed at Imperial prior to joining Amazon and is not associated with Amazon.

References

- B. L. Ammari, E. S. Johnson, G. Stinchfield, T. Kim, M. Bynum, W. E. Hart, J. Pulsipher, and C. D. Laird. Linear model decision trees as surrogates in optimization of engineering applications. *Computers & Chemical Engineering*, 178, 2023.
- R. Anderson, J. Huchette, W. Ma, C. Tjandraatmadja, and J. P. Vielma. Strong mixed-integer programming formulations for trained neural networks. *Mathematical Programming*, 183(1):3–39, 2020.
- K. Borgwardt, E. Ghisu, F. Llinares-López, L. O’Bray, B. Rieck, et al. Graph kernels: State-of-the-art and future challenges. *Foundations and Trends® in Machine Learning*, 13(5-6):531–712, 2020.
- K. M. Borgwardt and H.-P. Kriegel. Shortest-path kernels on graphs. In *International Conference on Data Mining*, 2005.
- A. Cheng, J. Wang, X. Zhang, Q. Chen, P. Wang, and J. Cheng. DPNAS: Neural architecture search for deep learning with differential privacy. *AAAI*, 2022.
- X. Dong and Y. Yang. NAS-Bench-201: Extending the scope of reproducible neural architecture search. In *ICLR*, 2020.
- T. Elsken, J. H. Metzen, and F. Hutter. Neural architecture search: a survey. *Journal of Machine Learning Research*, 2019.
- M. Fischetti and J. Jo. Deep neural networks and mixed integer linear optimization. *Constraints*, 23(3):296–309, 2018.
- R. W. Floyd. Algorithm 97: Shortest path. *Communications of the ACM*, 5(6):345–345, 1962.
- P. I. Frazier. A tutorial on Bayesian optimization. *arXiv preprint arXiv:1807.02811*, 2018.
- R. Garnett. *Bayesian Optimization*. Cambridge University Press, 2023.
- T. Gärtner, P. Flach, and S. Wrobel. On graph kernels: Hardness results and efficient alternatives. In *Learning Theory and Kernel Machines*, 2003.
- Gurobi Optimization, LLC. Gurobi optimizer reference manual, 2024. URL <https://www.gurobi.com>.
- C. Hojny, S. Zhang, J. S. Campos, and R. Misener. Verifying message-passing neural networks via topology-based bounds tightening. In *ICML*, 2024.
- J. Huchette, G. Muñoz, T. Serra, and C. Tsay. When deep learning meets polyhedral theory: A survey. *arXiv preprint arXiv:2305.00241*, 2023.
- Y. Jaafra, J. L. Laurent, A. Deruyver, and M. S. Naceur. Reinforcement learning for neural architecture search: A review. *Image and Vision Computing*, 89:57–66, 2019.
- K. Kandasamy, W. Neiswanger, J. Schneider, B. Póczos, and E. P. Xing. Neural architecture search with Bayesian optimisation and optimal transport. *NeurIPS*, 31, 2018.
- N. Kriege and P. Mutzel. Subgraph matching kernels for attributed graphs. In *ICML*, 2012.
- N. M. Kriege, P.-L. Giscard, and R. Wilson. On valid optimal assignment kernels and applications to graph classification. *NeurIPS*, 2016.
- N. M. Kriege, F. D. Johansson, and C. Morris. A survey on graph kernels. *Applied Network Science*, 5:1–42, 2020.
- C. Liu, B. Zoph, M. Neumann, J. Shlens, W. Hua, L.-J. Li, L. Fei-Fei, A. Yuille, J. Huang, and K. Murphy. Progressive neural architecture search. In *ECCV*, 2018.
- H. Liu, K. Simonyan, and Y. Yang. DARTS: Differentiable architecture search. In *ICLR*, 2019.
- A. G. d. G. Matthews, M. van der Wilk, T. Nickson, K. Fujii, A. Boukouvalas, P. León-Villagrà, Z. Ghahramani, and J. Hensman. GPflow: A Gaussian process library using TensorFlow. *Journal of Machine Learning Research*, 18(40):1–6, 2017.
- T. McDonald, C. Tsay, A. M. Schweidtmann, and N. Yorke-Smith. Mixed-integer optimisation of graph neural networks for computer-aided molecular design. *Computers & Chemical Engineering*, 185:108660, 2024.
- V. V. Mišić. Optimization of tree ensembles. *Operations Research*, 68(5):1605–1624, 2020.
- M. Mistry, D. Letsios, G. Krennrich, R. M. Lee, and R. Misener. Mixed-integer convex nonlinear optimization with gradient-boosted trees embedded. *INFORMS Journal on Computing*, 33(3):1103–1119, 2021.

- W. Neiswanger, K. Kandasamy, B. Poczos, J. Schneider, and E. Xing. ProBo: a framework for using probabilistic programming in Bayesian optimization. *arXiv preprint arXiv:1901.11515*, 2019.
- G. Nikolentzos, G. Siglidis, and M. Vazirgiannis. Graph kernels: A survey. *Journal of Artificial Intelligence Research*, 72:943–1027, 2021.
- Z. Qiu, W. Bi, D. Xu, H. Guo, H. Ge, Y. Liang, H. P. Lee, and C. Wu. Efficient self-learning evolutionary neural architecture search. *Applied Soft Computing*, 146:110671, 2023.
- E. Real, A. Aggarwal, Y. Huang, and Q. V. Le. Regularized evolution for image classifier architecture search. In *AAAI*, 2019.
- P. Ren, Y. Xiao, X. Chang, P.-Y. Huang, Z. Li, X. Chen, and X. Wang. A comprehensive survey of neural architecture search: Challenges and solutions. *ACM Computing Surveys*, 54(4):1–34, 2021.
- B. Ru, X. Wan, X. Dong, and M. Osborne. Interpretable neural architecture search via Bayesian optimisation with Weisfeiler-Lehman kernels. In *ICLR*, 2021.
- S. Salmani Pour Avval, N. D. Eskue, R. M. Groves, and V. Yaghoubi. Systematic review on neural architecture search. *Artificial Intelligence Review*, 58(3):73, 2025.
- E. Schulz, M. Speekenbrink, and A. Krause. A tutorial on Gaussian process regression: Modelling, exploring, and exploiting functions. *Journal of mathematical psychology*, 85, 2018.
- A. M. Schweidtmann, D. Bongartz, D. Grothe, T. Kerkenhoff, X. Lin, J. Najman, and A. Mitsos. Deterministic global optimization with Gaussian processes embedded. *Mathematical Programming Computation*, 13(3):553–581, 2021.
- N. Shervashidze, P. Schweitzer, E. J. Van Leeuwen, K. Mehlhorn, and K. M. Borgwardt. Weisfeiler-lehman graph kernels. *Journal of Machine Learning Research*, 12(9), 2011.
- H. Shi, R. Pi, H. Xu, Z. Li, J. Kwok, and T. Zhang. Bridging the gap between sample-based and one-shot neural architecture search with BONAS. *NeurIPS*, 2020.
- G. Siglidis, G. Nikolentzos, S. Limnios, C. Giatsidis, K. Skianis, and M. Vazirgiannis. GraKel: A graph kernel library in Python. *Journal of Machine Learning Research*, 21(54):1–5, 2020.
- J. Snoek, O. Rippel, K. Swersky, R. Kiros, N. Satish, N. Sundaram, M. Patwary, M. Prabhat, and R. Adams. Scalable Bayesian optimization using deep neural networks. In *ICML*, 2015.
- J. T. Springenberg, A. Klein, S. Falkner, and F. Hutter. Bayesian optimization with robust Bayesian neural networks. *NeurIPS*, 2016.
- N. Srinivas, A. Krause, S. Kakade, and M. Seeger. Gaussian process optimization in the bandit setting: No regret and experimental design. In *ICML*, 2010.
- A. Thebelt, J. Kronqvist, M. Mistry, R. M. Lee, N. Sudermann-Merx, and R. Misener. ENTMOOT: A framework for optimization over ensemble tree models. *Computers & Chemical Engineering*, 151:107343, 2021.
- A. Thebelt, J. Wiebe, J. Kronqvist, C. Tsay, and R. Misener. Maximizing information from chemical engineering data sets: Applications to machine learning. *Chemical Engineering Science*, 252:117469, 2022.
- C. Tsay, J. Kronqvist, A. Thebelt, and R. Misener. Partition-based formulations for mixed-integer optimization of trained ReLU neural networks. In *NeurIPS*, 2021.
- S. V. N. Vishwanathan, N. N. Schraudolph, R. Kondor, and K. M. Borgwardt. Graph kernels. *The Journal of Machine Learning Research*, 11:1201–1242, 2010.
- X. Wan, H. Kenlay, B. Ru, A. Blaas, M. Osborne, and X. Dong. Adversarial attacks on graph classifiers via Bayesian optimisation. In *NeurIPS*, 2021.
- X. Wan, P. Osselin, H. Kenlay, B. Ru, M. A. Osborne, and X. Dong. Bayesian optimisation of functions on graphs. *NeurIPS*, 2023.
- K. Wang, L. Lozano, C. Cardonha, and D. Bergman. Optimizing over an ensemble of trained neural networks. *INFORMS Journal on Computing*, 2023.
- W. Wen, H. Liu, Y. Chen, H. Li, G. Bender, and P.-J. Kindermans. Neural predictor for neural architecture search. In *ECCV*, 2020.
- C. White, W. Neiswanger, S. Nolen, and Y. Savani. A study on encodings for neural architecture search. In *NeurIPS*, 2020.
- C. White, W. Neiswanger, and Y. Savani. BANANAS: Bayesian optimization with neural architectures for neural architecture search. In *AAAI*, 2021a.

- C. White, S. Nolen, and Y. Savani. Exploring the loss landscape in neural architecture search. In *UAI*, 2021b.
- C. White, M. Safari, R. Sukthanker, B. Ru, T. Elsken, A. Zela, D. Dey, and F. Hutter. Neural architecture search: insights from 1000 papers. *arXiv preprint arXiv:2301.08727*, 2023.
- B. Wu, X. Dai, P. Zhang, Y. Wang, F. Sun, Y. Wu, Y. Tian, P. Vajda, Y. Jia, and K. Keutzer. FBNet: Hardware-aware efficient convnet design via differentiable neural architecture search. In *CVPR*, 2019.
- Y. Xie, S. Zhang, J. Paulson, and C. Tsay. Global optimization of Gaussian process acquisition functions using a piecewise-linear kernel approximation. *arXiv preprint arXiv:2410.16893*, 2024.
- Y. Xie, S. Zhang, J. Qing, R. Misener, and C. Tsay. BoGrape: Bayesian optimization over graphs with shortest-path encoded. *arXiv preprint arXiv:2503.05642*, 2025.
- C. Ying, A. Klein, E. Christiansen, E. Real, K. Murphy, and F. Hutter. NAS-Bench-101: Towards reproducible neural architecture search. In *ICML*, 2019.
- S. Zhang, J. S. Campos, C. Feldmann, D. Walz, F. Sandfort, M. Mathea, C. Tsay, and R. Misener. Optimizing over trained GNNs via symmetry breaking. In *NeurIPS*, 2023.
- S. Zhang, J. S. Campos, C. Feldmann, F. Sandfort, M. Mathea, and R. Misener. Augmenting optimization-based molecular design with graph neural networks. *Computers & Chemical Engineering*, 186:108684, 2024.
- B. Zoph and Q. Le. Neural architecture search with reinforcement learning. In *ICLR*, 2017.

A Shortest path encoding

A.1 Encoding

For each variable Var in Table 1, we use $Var(G)$ to denote its value on a given graph G . For example, $d_{u,v}(G)$ is the shortest distance from node u to node v in graph G . If graph G is given, all variable values can be easily obtained using classic shortest-path algorithms like the Floyd–Warshall algorithm (Floyd, 1962). However, for graph optimization, those variables need to be constrained properly so that they have correct values for any given graph. In this section, we first provide a list of necessary conditions that these variables should satisfy based on their definitions. Then we will prove that these conditions are sufficient in next section.

Condition (C1): At least n_0 nodes exist. W.l.o.g., assume that nodes with smaller indexes exist:

$$\begin{cases} \sum_{v \in [n]} A_{v,v} \geq n_0 \\ A_{v,v} \geq A_{v+1,v+1}, \quad \forall v \in [n-1] \end{cases}$$

Condition (C2): Initialization for nonexistent nodes, i.e., if either node u or node v does not exist, edge $u \rightarrow v$ cannot exist, node u cannot reach node v , and the shortest distance from node u to node v is infinity, i.e., n :

$$\min(A_{u,u}, A_{v,v}) = 0 \Rightarrow A_{u,v} = 0, r_{u,v} = 0, d_{u,v} = n, \forall u, v \in [n], u \neq v$$

which could be rewritten as the following linear constraints:

$$\begin{cases} 2 \cdot A_{u,v} \leq A_{u,u} + A_{v,v}, & \forall u, v \in [n], u \neq v \\ 2 \cdot r_{u,v} \leq A_{u,u} + A_{v,v}, & \forall u, v \in [n], u \neq v \\ d_{u,v} \geq n \cdot (1 - A_{u,u}), & \forall u, v \in [n], u \neq v \\ d_{u,v} \geq n \cdot (1 - A_{v,v}), & \forall u, v \in [n], u \neq v \end{cases}$$

Condition (C3): Initialization for single node, i.e., node v can reach itself with shortest distance as 0, and node v is obviously the only node that appears in the shortest path from node v to itself:

$$\begin{cases} r_{v,v} = 1, & \forall v \in [n] \\ d_{v,v} = 0, & \forall v \in [n] \\ \delta_{v,v}^v = 1, & \forall v \in [n] \\ \delta_{v,v}^w = 0, & \forall v, w \in [n], v \neq w \end{cases}$$

Condition (C4): Initialization for each edge, i.e., if edge $u \rightarrow v$ exists, node u can reach node v with shortest distance as 1. Otherwise, the shortest distance from node u to node v is larger than 1:

$$\begin{aligned} A_{u,v} = 1 &\Rightarrow r_{u,v} = 1, d_{u,v} = 1, \quad \forall u, v \in [n], u \neq v \\ A_{u,v} = 0 &\Rightarrow d_{u,v} > 1, \quad \forall u, v \in [n], u \neq v \end{aligned}$$

which could be rewritten as the following linear constraints:

$$\begin{cases} r_{u,v} \geq A_{u,v}, & \forall u, v \in [n], u \neq v \\ d_{u,v} \geq 2 - A_{u,v}, & \forall u, v \in [n], u \neq v \\ d_{u,v} \leq 1 + (n-1) \cdot (1 - A_{u,v}), & \forall u, v \in [n], u \neq v \end{cases}$$

Condition (C5): Compatibility between distance and reachability, i.e., node u can reach node v if and only the shortest distance from node u to node v is finite:

$$d_{u,v} < n \Leftrightarrow r_{u,v} = 1, \forall u, v \in [n], u \neq v$$

which could be rewritten as the following linear constraints:

$$\begin{cases} d_{u,v} \leq n - r_{u,v}, & \forall u, v \in [n], u \neq v \\ d_{u,v} \geq n - (n-1) \cdot r_{u,v}, & \forall u, v \in [n], u \neq v \end{cases}$$

Condition (C6): Compatibility between path and reachability, i.e., (i) if node w appears in the shortest path from node u to node v , then node u can reach node w , and node w can reach node v (the opposite is not always true), which means that node u can reach node v via node w :

$$\delta_{u,v}^w = 1 \Rightarrow r_{u,w} = r_{w,v} = 1 \Rightarrow r_{u,v} = 1, \forall u, v, w \in [n], u \neq v \neq w$$

which could be rewritten as the following linear constraints:

$$\begin{cases} r_{u,w} + r_{w,v} \geq 2 \cdot \delta_{u,v}^w, & \forall u, v, w \in [n], u \neq v \neq w \\ r_{u,v} \geq r_{u,w} + r_{w,v} - 1, & \forall u, v, w \in [n], u \neq v \neq w \end{cases}$$

Condition (C7): Construction of shortest path, i.e., (i) always assume that both node u and node v appear in the shortest path from node u to node v for well-definedness, (ii) if edge $u \rightarrow v$ exists or node u cannot reach node v , then no other nodes can appear in the shortest path from node u to node v , (iii) if edge $u \rightarrow v$ does not exist but node u can reach node v , then at least one node except for node u and node v will appear in the shortest path from node u to node v :

$$\begin{aligned} \delta_{u,v}^u &= \delta_{u,v}^v = 1, & \forall u, v \in [n], u \neq v \\ A_{u,v} = 1 \vee r_{u,v} = 0 &\Rightarrow \sum_{w \in [n]} \delta_{u,v}^w = 2, & \forall u, v \in [n], u \neq v \\ A_{u,v} = 0 \wedge r_{u,v} = 1 &\Rightarrow \sum_{w \in [n]} \delta_{u,v}^w > 2, & \forall u, v \in [n], u \neq v \end{aligned}$$

Observing that $A_{u,v} = 1 \vee r_{u,v} = 0 \Leftrightarrow r_{u,v} - A_{u,v} = 0$ since $r_{u,v} \geq A_{u,v}$ always holds, we can rewrite these constraints as the following linear constraints:

$$\begin{cases} \delta_{u,v}^u = \delta_{u,v}^v = 1, & \forall u, v \in [n], u \neq v \\ \sum_{w \in [n]} \delta_{u,v}^w \geq 2 + r_{u,v} - A_{u,v}, & \forall u, v \in [n], u \neq v \\ \sum_{w \in [n]} \delta_{u,v}^w \leq 2 + (n-2) \cdot (r_{u,v} - A_{u,v}), & \forall u, v \in [n], u \neq v \end{cases}$$

Condition (C8): Triangle inequality of shortest distance, i.e., if node u can reach node w and node w can reach node v , then the shortest distance from node u to node v is no larger than the shortest distance from node u to node w then to node v , and the equality holds when node w appears in the shortest path from node u to node v :

$$\begin{aligned} \delta_{u,v}^w = 1 &\Rightarrow d_{u,v} = d_{u,w} + d_{w,v}, & \forall u, v, w \in [n], u \neq v \neq w \\ r_{u,w} = r_{w,v} = 1 \wedge \delta_{u,v}^w = 0 &\Rightarrow d_{u,v} < d_{u,w} + d_{w,v}, & \forall u, v, w \in [n], u \neq v \neq w \end{aligned}$$

where we omit $r_{u,w} = r_{w,v} = 1$ in the first line since $\delta_{u,v}^w = 1$ implies it.

Similarly, we can rewrite these constraints as the following linear constraints:

$$\begin{cases} d_{u,v} \leq d_{u,w} + d_{w,v} - (1 - \delta_{u,v}^w) + (n+1) \cdot (2 - r_{u,w} - r_{w,v}), & \forall u, v, w \in [n], u \neq v \neq w \\ d_{u,v} \geq d_{u,w} + d_{w,v} - 2n \cdot (1 - \delta_{u,v}^w), & \forall u, v, w \in [n], u \neq v \neq w \end{cases}$$

Putting Conditions (C1)–(C8) together presents the final formulation Eq. (Graph-Encoding).

A.2 Theoretical guarantee

All constraints in Eq. (Graph-Encoding) are necessary conditions, i.e., as shown in Lemma 1.

Lemma 1. *Given any labeled graph G with n nodes, $\{A_{u,v}(G), r_{u,v}(G), d_{u,v}(G), \delta_{u,v}^w(G)\}_{u,v,w \in [n]}$ is a feasible solution of Eq. (Graph-Encoding) with $n_0 = n$.*

Proof. By definition, it is easy to check that $\{A_{u,v}(G), r_{u,v}(G), d_{u,v}(G), \delta_{u,v}^w(G)\}_{u,v,w \in [n]}$ satisfies condition (C1)–(C8). \square

The opposite is non-trivial to prove, that is, any feasible solution of Eq. (Graph-Encoding) corresponds to an unique graph with $\sum_{v \in [n]} A_{v,v}$ nodes, which is guaranteed by Theorem 1.

Proof of Theorem 1. Denote $\mathcal{F}_{n_0,n}$ as the feasible domain restricted by Eq. (Graph-Encoding) with size $[n_0, n]$, and $\mathcal{G}_{n_0,n}$ as the whole graph space with node numbers in $[n_0, n]$. Define the following mapping:

$$\begin{aligned} \mathcal{M}_{n_0,n} : \mathcal{F}_{n_0,n} &\rightarrow \mathcal{G}_{n_0,n} \\ \{A_{u,v}, r_{u,v}, d_{u,v}, \delta_{u,v}^w\}_{u,v,w \in [n]} &\mapsto \{A_{u,v}\}_{u,v \in [n]} \end{aligned}$$

For simplicity, we still use a $n \times n$ adjacency matrix to define a graph with node number less than n and use $A_{v,v}(G)$ to represent the existence of node v . Also, the subscriptions, e.g., $\{u,v,w \in [n]\}$, are omitted from now on.

If $n_1 = \sum_{v \in [n]} A_{v,v} < n$, Condition (C1) forces that:

$$A_{v,v} = \begin{cases} 1, & v \in [n_1] \\ 0, & v \in [n] \setminus [n_1] \end{cases}$$

For any pair of (u, v) with $u \neq v$ and $\max(u, v) \geq n_1$, Conditions (C2) and (C7) uniquely define $\{r_{u,v}, d_{u,v}, \delta_{u,v}^w\}$ as:

$$r_{u,v} = 0, d_{u,v} = n, \delta_{u,v}^w = \begin{cases} 1, & w \in \{u, v\} \\ 0, & w \notin \{u, v\} \end{cases}$$

Therefore, it is equivalent to show that $\mathcal{M}_{n,n}$ is a bijection. Since Lemma 1 already shows that $\mathcal{M}_{n,n}$ is a surjection, it suffices to prove that $\mathcal{M}_{n,n}$ is an injection. Precisely, for any feasible solution $\{A_{u,v}, r_{u,v}, d_{u,v}, \delta_{u,v}^w\}$, there exists a graph G with adjacency matrix given by $\{A_{u,v}(G)\} = \{A_{u,v}\}$, such that:

$$\{r_{u,v}(G), d_{u,v}(G), \delta_{u,v}^w(G)\} = \{r_{u,v}, d_{u,v}, \delta_{u,v}^w\} \quad (\star)$$

Since $r_{v,v}(G), d_{v,v}(G), \delta_{v,v}^w(G), \delta_{u,v}^u(G), \delta_{u,v}^v(G)$ are defined for completeness of our definition, whose variable counterparts are properly and uniquely defined in Condition (C3) and the first part of Condition (C7), we only need to consider all triples (u, v, w) with $u \neq v \neq w$, which will not be specified later for simplicity.

Now we are going to prove Eq. (\star) holds by induction on $\min(d_{u,v}(G), d_{u,v}) < n$.

When $\min(d_{u,v}(G), d_{u,v}) = 1$, for any pair of (u, v) , we have:

$$\begin{aligned} d_{u,v}(G) = 1 &\Rightarrow A_{u,v}(G) = 1, r_{u,v}(G) = 1, \delta_{u,v}^w(G) = 0 && \leftarrow \text{definition} \\ &\Rightarrow A_{u,v} = 1 && \leftarrow \text{definition of } \mathcal{M}_{n,n} \\ &\Rightarrow r_{u,v} = 1, d_{u,v} = 1, \delta_{u,v}^w = 0 && \leftarrow \text{Conditions (C4) + (C7)} \end{aligned}$$

and:

$$\begin{aligned} d_{u,v} = 1 &\Rightarrow A_{u,v} = 1, r_{u,v} = 1, \delta_{u,v}^w = 0 && \leftarrow \text{Conditions (C4) + (C7)} \\ &\Rightarrow A_{u,v}(G) = 1 && \leftarrow \text{definition of } \mathcal{M}_{n,n} \\ &\Rightarrow r_{u,v}(G) = 1, d_{u,v}(G) = 1, \delta_{u,v}^w(G) = 0 && \leftarrow \text{definition} \end{aligned}$$

For both cases, we have Eq. (\star) holds.

Assume that Eq. (\star) holds for any pair of (u, v) with $\min(d_{u,v}(G), d_{u,v}) \leq sd$ with $sd < n - 1$. Consider the following two cases for $\min(d_{u,v}(G), d_{u,v}) = sd + 1 < n$.

Case I: If $d_{u,v}(G) = sd + 1$, we know that $r_{u,v}(G) = 1$ since the shortest distance from node u to node v is finite. For any $w \notin \{u, v\}$ such that $\delta_{u,v}^w(G) = 1$, we have:

$$\begin{aligned} \delta_{u,v}^w(G) = 1 &\Rightarrow d_{u,w}(G) + d_{w,v}(G) = d_{u,v}(G) && \leftarrow \text{definition of } \delta_{u,v}^w(G) \\ &\Rightarrow \max(d_{u,w}(G), d_{w,v}(G)) \leq sd && \leftarrow d_{u,w}(G) > 0, d_{w,v}(G) > 0 \\ &\Rightarrow d_{u,w} = d_{u,w}(G), d_{w,v} = d_{w,v}(G) && \leftarrow \text{assumption of induction} \\ &\Rightarrow r_{u,w} = r_{w,v} = 1 && \leftarrow \text{Condition (C5)} \\ &\Rightarrow d_{u,v} \leq d_{u,w} + d_{w,v} = sd + 1 && \leftarrow \text{Condition (C8)} \\ &\Rightarrow d_{u,v} = sd + 1 && \leftarrow d_{u,v} \geq sd + 1 \\ &\Rightarrow r_{u,v} = 1, \delta_{u,v}^w = 1 && \leftarrow \text{Conditions (C5) + (C8)} \end{aligned}$$

which means that $r_{u,v} = r_{u,v}(G)$, $d_{u,v} = d_{u,v}(G)$, $\delta_{u,v}^w = \delta_{u,v}^w(G)$ with $\delta_{u,v}^w(G) = 1$.

For any $w \notin \{u, v\}$ such that $\delta_{u,v}^w(G) = 0$. If $\delta_{u,v}^w = 1$, then we have:

$$\begin{aligned} \delta_{u,v}^w = 1 &\Rightarrow r_{u,w} = r_{w,v} = 1, d_{u,v} = d_{u,w} + d_{w,v} && \leftarrow \text{Conditions (C6) + (C8)} \\ &\Rightarrow \max(d_{u,w}, d_{w,v}) \leq sd && \leftarrow d_{u,w} > 0, d_{w,v} > 0 \\ &\Rightarrow d_{u,w}(G) = d_{u,w}, d_{w,v}(G) = d_{w,v} && \leftarrow \text{assumption of induction} \\ &\Rightarrow d_{u,w}(G) + d_{w,v}(G) = sd + 1 = d_{u,v}(G) && \leftarrow d_{u,v}(G) = d_{u,v} = sd + 1 \\ &\Rightarrow \delta_{u,v}^w(G) = 1 && \leftarrow \text{definition of } \delta_{u,v}^w(G) \end{aligned}$$

which contradicts to $\delta_{u,v}^w(G) = 0$. Thus $\delta_{u,v}^w = 0 = \delta_{u,v}^w(G)$ with $\delta_{u,v}^w(G) = 0$.

Case II: If $d_{u,v} = sd + 1$, from $sd + 1 > 1$ and Condition (C4) we know that $A_{u,v} = 0$, from Condition (C5) we have $r_{u,v} = 1$, and then from Condition (C7) we obtain that $\sum_{w \in [n]} \delta_{u,v}^w > 2$.

For any $w \notin \{u, v\}$ such that $\delta_{u,v}^w = 1$, we have:

$$\begin{aligned}
 \delta_{u,v}^w = 1 &\Rightarrow d_{u,w} + d_{w,v} = d_{u,v} = sd + 1 && \leftarrow \text{Condition (C8)} \\
 &\Rightarrow \max(d_{u,w}, d_{w,v}) \leq sd && \leftarrow d_{u,w} > 0, d_{w,v} > 0 \\
 &\Rightarrow d_{u,w}(G) = d_{u,w}, d_{w,v}(G) = d_{w,v} && \leftarrow \text{assumption of induction} \\
 &\Rightarrow d_{u,v}(G) \leq d_{u,w}(G) + d_{w,v}(G) = sd + 1 && \leftarrow \text{definition of } d_{u,v}(G) \\
 &\Rightarrow d_{u,v}(G) = sd + 1 && \leftarrow d_{u,v}(G) \geq sd + 1 \\
 &\Rightarrow r_{u,v}(G) = 1, \delta_{u,v}^w(G) = 1 && \leftarrow \text{definition}
 \end{aligned}$$

which means that $r_{u,v}(G) = r_{u,v}$, $d_{u,v}(G) = d_{u,v}$, $\delta_{u,v}^w(G) = \delta_{u,v}^w$ with $\delta_{u,v}^w = 1$.

For any $w \notin \{u, v\}$ such that $\delta_{u,v}^w = 0$. If $\delta_{u,v}^w(G) = 1$, then we have:

$$\begin{aligned}
 \delta_{u,v}^w(G) = 1 &\Rightarrow d_{u,v}(G) = d_{u,w}(G) + d_{w,v}(G) && \leftarrow \text{definition of } \delta_{u,v}^w(G) \\
 &\Rightarrow \max(d_{u,w}(G), d_{w,v}(G)) \leq sd && \leftarrow d_{u,w}(G) > 0, d_{w,v}(G) > 0 \\
 &\Rightarrow d_{u,w} = d_{u,w}(G), d_{w,v} = d_{w,v}(G) && \leftarrow \text{assumption of induction} \\
 &\Rightarrow d_{u,w} + d_{w,v} = sd + 1 = d_{u,v} && \leftarrow d_{u,v}(G) = d_{u,v} = sd + 1 \\
 &\Rightarrow \delta_{u,v}^w = 1 && \leftarrow \text{Condition (C8)}
 \end{aligned}$$

which contradicts to $\delta_{u,v}^w = 0$. Thus $\delta_{u,v}^w(G) = 0 = \delta_{u,v}^w$ with $\delta_{u,v}^w = 0$.

The remaining case is $d_{u,v}(G) = d_{u,v} = n$, i.e., node u cannot reach node v . It is straightforward to verify that:

$$\begin{aligned}
 r_{u,v} = 0 &= r_{u,v}(G) && \leftarrow \text{Condition (C5), definition of } r_{u,v}(G) \\
 \delta_{u,v}^w = 0 &= \delta_{u,v}^w(G) && \leftarrow \text{Condition (C7), definition of } \delta_{u,v}^w(G)
 \end{aligned}$$

Therefore, Eq. (★) always holds, which completes the proof. \square

B Kernel encoding

This section presents encoding for shortest-graph kernels and binary node labels proposed in (Xie et al., 2025). Notations are slightly changed to keep consistency with this paper.

Graph kernel encoding Introduce indicator variables $p_{s,l_1,l_2}^{u,v} = \mathbf{1}(F_{u,l_1} = 1, d_{u,v} = s, F_{v,l_2} = 1)$ and count the number of each type of paths as:

$$P_{s,l_1,l_2}(G^i) = \sum_{u,v \in [N]} p_{s,l_1,l_2}^{u,v}.$$

Then SP kernel (k_g) could be formulated as:

$$\begin{aligned}
 k_g(G, G^i) &= \frac{1}{n^2 n_i^2} \sum_{s \in [n], l_1, l_2 \in [L_n]} P_{s,l_1,l_2}(G^i) \cdot P_{s,l_1,l_2}, \\
 k_g(G, G) &= \frac{1}{n^4} \sum_{s \in [n], l_1, l_2 \in [L_n]} P_{s,l_1,l_2}^2.
 \end{aligned}$$

To handle the quadratic term P_{s,l_1,l_2}^2 , we further introduce indicator variables $P_{s,l_1,l_2}^c = \mathbf{1}(P_{s,l_1,l_2} = c)$, and rewrite $k_g(G, G)$ as the following linear form:

$$k_g(G, G) = \frac{1}{n^4} \sum_{s \in [n], l_1, l_2 \in [L_n], c \in [n^2+1]} c^2 \cdot P_{s,l_1,l_2}^c.$$

Before formulating indicators $p_{s,l_1,l_2}^{u,v}$, we need indicators $d_{u,v}^s = \mathbf{1}(d_{u,v} = s)$ that satisfy:

$$\sum_{s \in [n+1]} d_{u,v}^s = 1, \quad \sum_{s \in [n+1]} s \cdot d_{u,v}^s = d_{u,v}, \quad \forall u, v \in [n],$$

using which we can formulate $p_{s,l_1,l_2}^{u,v}$, $\forall u, v, s \in [n]$, $l_1, l_2 \in [L_n]$ as:

$$3 \cdot p_{s,l_1,l_2}^{u,v} \leq F_{u,l_1} + d_{u,v}^s + F_{v,l_2}, \quad p_{s,l_1,l_2}^{u,v} \geq F_{u,l_1} + d_{u,v}^s + F_{v,l_2} - 2.$$

Similar to $d_{u,v}^s$, indicators P_{s,l_1,l_2}^c can be expressed as:

$$\sum_{c \in [n^2+1]} P_{s,l_1,l_2}^c = 1, \quad \sum_{c \in [n^2+1]} c \cdot P_{s,l_1,l_2}^c = P_{s,l_1,l_2}, \quad \forall s \in [n], \quad l_1, l_2 \in [L_n].$$

Node label encoding k_n could be defined in multiple ways, Xie et al. (2025) propose the following permutational-invariant kernel measuring the pair-wise similarity among node features:

$$k_n(F_n^1, F_n^2) := \frac{1}{n_1 n_2 L_n} \sum_{v_1 \in [n_1], v_2 \in [n_2]} F_{v_1}^1 \cdot F_{v_2}^2 = \frac{1}{n_1 n_2 L_n} \sum_{l \in [L_n]} N_l(F_n^1) \cdot N_l(F_n^2),$$

where $N_l = \sum_{v \in [n]} F_{v,l}$, $\forall l \in [L_n]$, and $n_1 n_2 L_n$ is the normalized coefficient.

Similar to the graph kernel encoding, we have:

$$k_n(F_n, F_n^i) = \frac{1}{n n_i L_n} \sum_{l \in [L_n]} N_l(F_n^i) \cdot N_l,$$

$$k_n(F_n, F_n) = \frac{1}{n^2 L_n} \sum_{l \in [L_n]} N_l^2 = \frac{1}{n^2 L_n} \sum_{l \in [L_n], c \in [n+1]} c^2 \cdot N_l^c,$$

where indicators $N_l^c = \mathbf{1}(N_l = c)$ satisfy:

$$\sum_{c \in [n+1]} N_l^c = 1, \quad \sum_{c \in [n+1]} c \cdot N_l^c = N_l, \quad \forall l \in [L_n].$$

C Experimental details and full results

C.1 Hyperparameter settings in GP and BO

We implement our graph kernels defined in Eqs. (linear) and (exponential) as an inherited `Kernel` class in GPflow (Matthews et al., 2017). The initial values of the trainable kernel parameters α, β, γ and σ_k^2 are set to 1 with bounds $[0.01, 100]$. In BO, we apply a batch setting to return 5 architectures with the lowest LCB values in each iteration by setting Gurobi parameter `PoolSearchMode=2`. The final MIP model Eq. (Graph-Encoding) is designed for fixed graph size, but NAS-Bench-101 dataset consists of graph sizes ranging from 2 to 7. Our graph encoding supports changeable sizes. The only issue is that the normalized coefficients in kernel encoding are no longer constant, which complicates our formulation. One can resolve this issue by replacing these coefficients by constants or ignoring them. In NAS, however, architectures with more nodes usually have better performance. For instance, most high-quality architectures in NAS-Bench-101 have either 6 or 7 nodes. Therefore, in our experiments for NAS-Bench-101, we simply solve two MIP models with graph size set to $N = 6, 7$ sequentially. Each model returns 5 architectures, we still select 5 of 10 with the lowest LCB values. To encourage exploration, we set $\beta_t^{1/2} = 3$ in LCB. The `TimeLimit` parameter in Gurobi for solving each MIP is set as 1800s.

C.2 Details on baselines

We provide more details on algorithms used in Section 4.2. We adapt the implementation from (White et al., 2020) for all baselines except for NAS-BOWL, where we use the publicly available code from (Ru et al., 2021).

- **Random:** Randomly sample the required number of architectures and evaluate them.
- **DNGO:** Deep Network for Global Optimization (DNGO) uses neural networks to learn an adaptive set of basis functions for Bayesian linear regression instead of GP in BO. It is adapted for NAS by treating the adjacency matrix of graph as encoding vector inputs.
- **BOHAMIANN:** Bayesian Optimization with Hamiltonian Monte Carlo Artificial Neural Networks (BO-HAMIANN) uses Bayesian neural networks as the surrogate model in both single- and multi-task BO, and achieves scalability through stochastic gradient Hamiltonian Monte Carlo. It is not originally designed for NAS but could be adapted by encoding graph input by adjacency matrix.

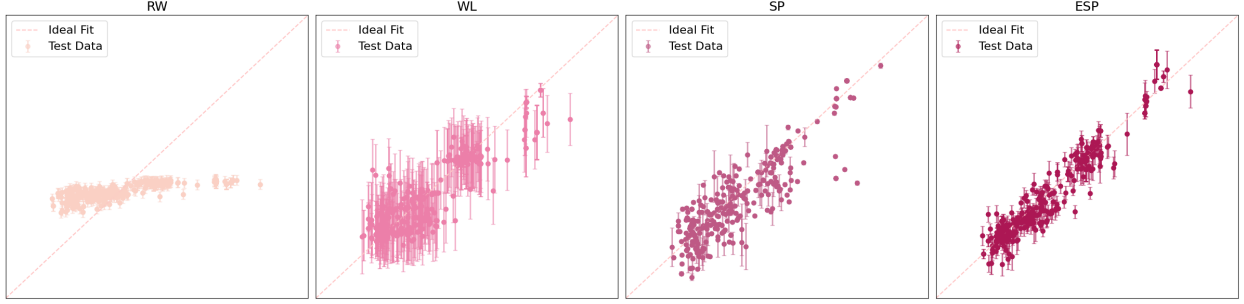


Figure 4: Predictive performance of graph GPs with different kernels. 50 and 400 architectures are randomly sampled from NAS-Bench-101 for training and testing resp. Predicted deterministic validation error are plotted against the true values, with one standard deviation as error bars.

- **NASBOT:** Neural Architecture Search with Bayesian Optimisation and Optimal Transport (NASBOT) is a GP-based BO framework for NAS. It defines a distance metric to reveal the similarity between graphs called Optimal Transport Metrics for Architectures of Neural Networks (OTMANN). NASBOT specifically provides a list of operations for the evolutionary algorithm used in the acquisition function optimization.
- **Evolution:** Regularized evolution consists of mutating the best architectures from the population until a given budget runs out. White et al. (2020) set the population size to 30 and outdate the architecture with the worst validation accuracy instead of the oldest one because it results in better performance in NAS tasks following.
- **GP-BAYESOPT:** Standard BO with GP surrogate and UCB acquisition, implemented using ProBO (Neiswanger et al., 2019). Similarity (distance) metric between two architectures is defined as the sum of Hamming distances between the adjacency matrices and the associated operations.
- **GCN:** Use Graph Convolutional Networks (GCN) as the neural predictor to predict the performance of random architectures and select the best K samples for evaluation.
- **BONAS:** Bayesian Optimized Neural Architecture Search (BONAS) uses a GCN as surrogate model in BO to select multiple architectures in each iteration, and apply weight-sharing during the model training to accelerate traditional sampling methods.
- **Local search:** The simplest hill-climbing local search method evaluates all architectures in the neighborhood of a given sample. It is verified by White et al. (2021b) that local search is a strong baseline in NAS when the noise in the benchmark datasets is reduced to a minimum.
- **BANANAS:** Bayesian optimization with neural architectures for NAS (BANANAS) uses a meta neural network over path encoding of individual architectures to predict the validation accuracies. The trained meta NN is used as the surrogate model in BO.
- **NAS-BOWL:** NAS-BOWL is a BO-based NAS algorithm which uses Weisfeiler Lehman (WL) graph kernel in GP surrogate model and adapts to both random sampling and mutation for optimizing the expected improvement (EI) acquisition function. Their experiment results show better performance of NAS-BOWL when using mutation as the acquisition function solver, hence we choose this setting to compare against. NAS-BOWL is considered as the state-of-the-art NAS algorithm.

C.3 Additional graph BO for NAS results

We present additional experiment results on comparing NAS-GOAT with baselines when performing graph BO on NAS-Bench-101 and NAS-Bench-201 benchmarks. Figure 5 shows the performance of the remaining baselines in deterministic setting, where NAS-GOAT still outperforms others in all cases. Figure 6 summarizes the comparisons between NAS-GOAT and all 11 baselines in noisy setting. NAS-GOAT demonstrates comparable performance as state-of-the-art baselines, e.g. NAS-BOWL, NASBOT, BONAS. Note that the “noisy” setting is not another optimization task with noisy function evaluations, where we need to show NAS-GOAT still achieves the best objective function values. Instead, it is a NAS-specific setting where a good NAS algorithm is expected to find architectures with promising test accuracy even with unstable validation accuracy due to stochasticity in training process.

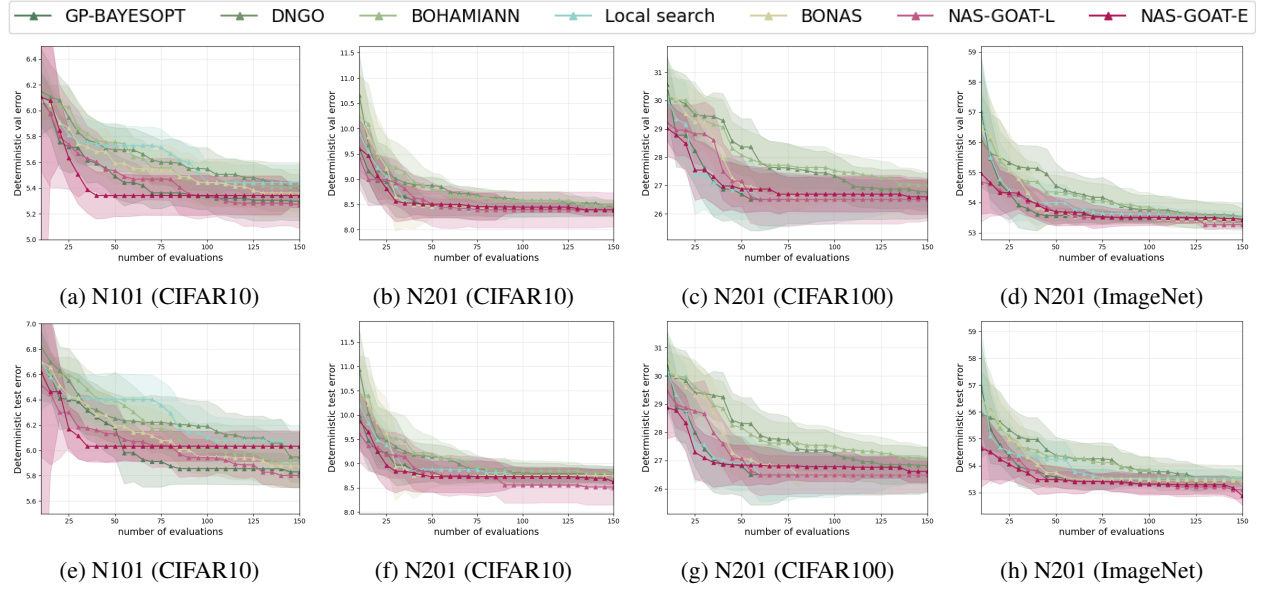


Figure 5: Comparison NAS-GOAT with the remaining baselines. Numerical results of Graph BO on NAS-Bench-101 (N101) and NAS-Bench-201 (N201). **(Top)** Deterministic validation error. **(Bottom)** The corresponding test error. Median with one standard deviation over 20 replications is plotted.

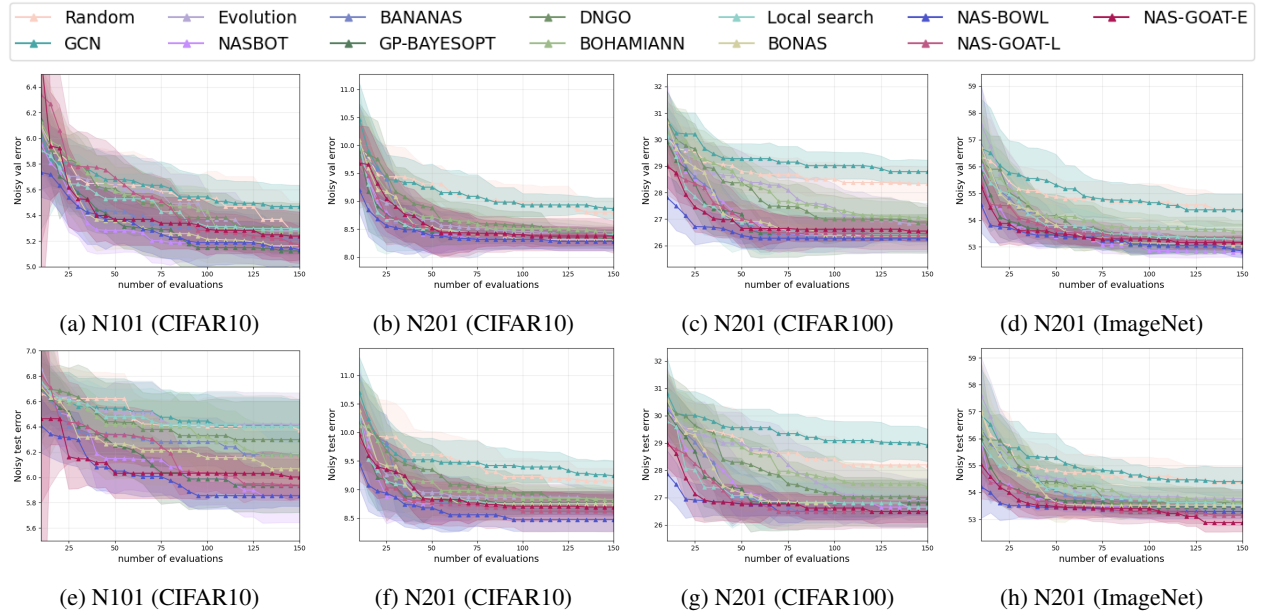


Figure 6: Numerical results of Graph BO on NAS-Bench-101 (N101) and NAS-Bench-201 (N201). **(Top)** Noisy validation error. **(Bottom)** The corresponding test error. Median with one standard deviation over 20 replications is plotted.